Quantifying the spreading factor to compare the wetting properties of minerals at molecular level – case study: sphalerite surface

Mehdi Mohseni [1], Mahmoud Abdollahy [1], Reza Poursalehi [2], Mohammad Reza Khalesi [1]

[1] Tarbiat Modares University, Faculty of Engineering & Technology, Department of Mining Engineering, Tehran, Iran
[2] Tarbiat Modares University, Faculty of Engineering & Technology, Department of Materials Engineering, Tehran, Iran

Corresponding author: E-mail address: minmabd@modares.ac.ir (M. Abdollahy)

Abstract: Spreading of water droplet on sphalerite surface was quantified at molecular level and was utilized for comparison of the wetting properties of sphalerite protonated and hydroxylated surfaces. Molecular dynamic simulations were used to characterize the wetting of sphalerite (110) plane. Experimental contact angles of water droplet on sphalerite surfaces were measured and the results were compared with simulated contact angles to ensure that the simulations are accurate enough for calculation of spreading factors. Shape descriptors such as perimeter, area, Feret's diameters and circularity were used to characterize the shape of droplet-sphalerite interface at molecular level. Using the shape descriptors, different spreading factors were defined and calculated spreading factors were correlated with simulated contact angle. It was shown that spreading factors which were defined as the volume of water droplet divided by the area and Feret's diameters, with correlation coefficient of 0.98 and 0.97, can be used as accurate tools for wetting comparison of functionalized sphalerite surface at molecular scale. Proposed approach also can be used for investigations on the effect of surface chemical and physical anisotropies on preferred wetting in specific direction at molecular scales.

Keywords: Wettability, contact angle, molecular simulation, sphalerite, spreading factor

1. Introduction

Wetting of a liquid on a solid surface is important for a wide range of scientific and industrial processes. Capillary actions in plants, ink spreading, mass transfer in porous media are some of manifold application of the wetting phenomena (Carré and Eustache, 2000; Ehlers and Goss, 2016; Prat, 2007). Wetting also plays a key role in powder technologies and especially in flotation process (Chau et al., 2009). Contact angle measurement as the main and usual method for quantifying the wetting properties of surface has been presented by Young equation (De Gennes et al., 2013; Ferrari et al., 2012; Yuan and Lee, 2013). Solid surface with water contact angle less than 90 degrees is called hydrophilic otherwise, the surface is called hydrophobic (Krasowska et al., 2009). In general, hydrophilicity and hydrophobicity represents the same feature of materials: ''Wetting''; but pointing in opposite directions.

Experimental and calculation methods have been used to measure the contact angle of water on specific surfaces in different fields of study. Traditionally, experimental approaches such as sessile drop, captive bubble, capillary rise, Wilhelmy plate and Washburn methods have been widely used in measurement of contact angle (Chau, 2009; Yuan and Lee, 2013). Recently, an increased interest has been shown in using molecular dynamic (MD) simulation for estimation of the contact angle at molecular scale (Do Hong et al., 2009; Du and Miller, 2007; Fan and Cağin, 1995; Kalinichev et al., 2007; Koishi et al., 2011; Park et al., 2011; Shahraz et al., 2013; Werder et al., 2001; Yan et al., 2013). Since contact angle of a surface is balance between adhesive (liquid to solid) and cohesive (liquid to liquid) forces through intermolecular interaction (Pawlik, 2008), evaluating the wetting properties of materials, from molecular point of view, is especially important. MD simulations coupled to

experimental results are capable to provide a new perspective and deep insight into the structure and dynamics of mineral - aqueous systems (Cygan and Kubicki, 2001; Frenkel and Smit, 2001; Kalinichev, 2014). Providing the molecular scale information about the structure and characteristics of mineral – aqueous interface can be used to explain how a molecular scale interaction results in a macroscopic observation.

In many of MD simulation based studies estimation of contact angle for a nano droplet on the substrate has been used for wetting estimation of surface at molecular scale. C. F. Fan and T.Cagin (Fan and Cağin, 1995) simulated the contact angle of water and methylene iodide at crystalline surface of polyethylene, polytetrafluoroethylene and polyethylene terephthalate; they found an agreement between experimental and simulated contact angle trend. S. D. Hong et al, used the MD simulations for evaluation of the increasing characteristic energy on static and dynamic contact angle of water droplet on a solid surface; they found that the static contact angle and hysteresis of dynamic contact angle increases with increasing characteristic energy (Do Hong et al., 2009). Obtained results from MD simulation of water contact angle on α-quartz, orthoclase and muscovite, as common minerals in sand and silt fractions, have been shown a good agreement with experimental contact angle measurements (Zhang et al., 2016). J. Jin et al, used the MD simulation for calculation of water contact angle on sphalerite (ZnS), villimaninite (CuS_2), covellit (CuS) and copper-zinc sulfide ($CuZnS_2$) minerals and investigation on the hydrophobicity of Cu^{2+} activated sphalerite; they clarified that the activation of sphalerite with copper ion make the surface more hydrophobic than the fresh sphalerite surface (Jin et al., 2015).

Because the conventional contact angle becomes ill-defined at the molecular level (Chen et al., 2014), calculation of contact angle from MD simulation results needs to a post processing procedures. To date, various methods have been developed and introduced to measure contact angle from MD simulations results. Hautman and Klein gave the following equation for calculation of contact angle from MD simulation results (Fan and Cağin, 1995):

$$Z_{c.m.} = (2)^{-4/3} R_0 \left(\frac{1-\cos\theta}{2+\cos\theta}\right)^{1/3} \left(\frac{3+\cos\theta}{2+\cos\theta}\right) \tag{1}$$

where θ is the contact angle, $Z_{c.m.}$ is the average height of the center of mass of droplet on the surface, R_0 is the radius of spherical drop of water. This method is applicable for both intersected sphere and irregular shape droplet. Fan and Cagin proposed their methodology based on the spherical geometry calculation of liquid droplet on mineral surface (Fan and Cağin, 1995); the contact angle defined as:

$$\cos\theta = 1 - \frac{h}{R} \tag{2}$$

where θ is the contact angle, h is the height of the droplet and R is the radius of fitted sphere to the liquid droplet. Refer to (Fan and Cağin, 1995) for more detailed information about the geometry calculation. Density field method has been widely used for contact angle calculation from MD simulation. In this method the droplet periphery is defined with density contours and contact angle directly is calculated from the shape of liquid droplet (Do Hong et al., 2009; Yan et al., 2013; Zhang et al., 2016).

Although evidence indicates the usability of above approaches in estimation of contact angle at molecular scale, there are some challenges with calculating of contact angle from MD simulation result. One of the greatest challenges is the spherical or circular assumption of liquid droplet on the surface; in molecular scale the liquid droplet finds an irregular shape and this fact cause the error in geometric parameters of fitted sphere or circle (Chen et al., 2014). Liquid droplet forms an irregular shape and the liquid-solid interface finds a preferred orientation in specific direction (Yuan and Zhao, 2013). This behavior is usually neglected for calculation of contact angle. In some studies, only the mean value from two perpendicular directions is reported for the overall surface contact angle (Jin et al., 2015). Another significant challenge is the effect of droplet size on estimated contact angle. In several reviewed studies, the reported values for contact angle have been affected by the droplet size (Do Hong et al., 2009; Wu et al., 2012), while in another study it has been proposed that in the size range from 850 to 1700 water molecules droplet size doesn't have much effect on simulated contact angle (Jin et al., 2015). Another challenge is neglecting the effect of liquid layer near the solid surface in conventional estimation methods of contact angle. In many of studies it has been proposed that the calculations must be considered at least 3 times of water molecular diameter from the surface to avoid

the influence of density fluctuations near the liquid-solid interface (Do Hong et al., 2009; Yan et al., 2013; Zhang et al., 2016); As mentioned, the wettability of surface arised from balance between adhesion and cohesion forces. At liquid-solid interface the liquid molecules are strongly attracted to the surface due to the adhesion forces; therefore, these molecules form a thin wetting layer on mineral surface and can plays an important role in surface wetting.

In this work, we adopt an alternative approach to estimate the wetting properties of a surface at molecular level. We propose a spreading factor based on the shape characteristics of the droplet-substrate interface. This method successfully was applied to wetting studies of sphalerite (110) surface and obtained results were confirmed by the simulated and experimental contact angle. The investigations have been done in the following way: firstly, the experimental contact angle of sphalerite was measured in different pHs and the results were compared with the calculated contact angle from MD simulation results. After that the shape of droplet-surface interface were characterized by using some shape descriptors such as area, perimeter, Ferret's diameters and circularity. Different spreading factors were then defined as criteria for comparison of surface wettability. Finally, best definition of spreading factor at molecular level was selected and proposed to compare the hydrophobicity of different surfaces. Fast estimation and accurate approximation in wetting properties of surface can account for the main differences of using spreading factor in comparison with the conventional contact angle methods in molecular simulations.

2. Materials and methods

We choose a case study approach to evaluate the appliance of spreading factor in wetting characterization of surface at molecular scale. Sphalerite (ZnS) mineral was selected as a substrate for experimental and simulated contact angle measurements. We applied conventional experimental and simulation approaches for investigation on the effect of functional groups on wetting behavior of sphalerite in macro and nano scale, respectively. Spreading factors in molecular scale were defined as the droplet's volume divided by shape characteristics of interface such as area, perimeter and Ferret's diameters of water-sphalerite (110) interface for each system. Results from spreading factors calculation were correlated with simulated contact angles and best definition for spreading factor was proposed. The procedures are detailed as following.
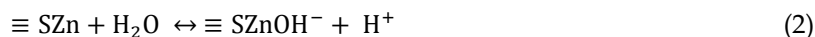
2.1 Experimental

Synthetic pure sphalerite was mounted in epoxy resin while a free flat surface was released for any modifications and measurements. Contact angles were measured using sessile drop method(Chau, 2009; Yuan and Lee, 2013). Before every measurement, the sphalerite surface was conditioned in aqueous solution with specific pHs. Soft abrading with abrasive paper and dry polishing with polishing cloths before conditioning step were used to reduce the effect of any surface oxidation on the measurement. Polishing cloth was very soft woven wool cloth with high quality which usually used in final polishing step of minerals, glass, ferrous and nonferrous metals. Sodium hydroxide with a purity of 98% and hydrochloric acid with the purity of 37%, all from Merck Company were used for any pH adjustments. DI water was used in all experiments. All glassware was soaked in water-detergent solution and rinsed several times with distilled and DI water and dried in oven prior to use.

2.2 Simulation

All simulations were performed using the Forcite module. Molecular structure of sphalerite unit cell from American Mineralogist Crystal Structure Database (AMCSD) was used to model construction (Skinner, 1961). Because the sphalerite has a perfect cleavage in (110) plane all simulations were performed on this plane (Jin et al., 2015; Skinner, 1961). Potential models from Dreiding forcefield (Mayo et al., 1990) and charge equilibrium (QEq) were used for atomic interactions potential and charge distribution, respectively. In Dreiding forcefield, the potential energy includes non-bonded and bonded energies. Bond, angle, torsion and inversion energies are considered as bonded and electrostatic interactions, van der Waals and hydrogen bonding energies are considered as non-

bonded terms. Dreiding forcefield energy terms and parameters for Zn and S atoms are reported in Table 1.

In all MD simulations, typical values for different parameters were applied. The Ewald method and atom-based cutoff of 12.5 Å were used to treat electrostatic and van der Waals interactions, respectively. Berendsen thermostat and Andersen barostat were used for temperature and pressure control in NPT (fixed number, pressure and temperature) ensemble and Berendsen thermostat was used in NVT (fixed number, volume and temperature) ensemble. A sphalerite slab with size of 92×89 angstroms was constructed from 4 layers of (110) plane. Sphalerite surface protonated in acidic pHs and hydroxylated in alkaline pHs according to the reactions below (Forsling and Sun, 1997; Wang et al., 2011; Zhang et al., 1995):

$$\equiv ZnS + H^+ \leftrightarrow \equiv ZnSH^+ \tag{1}$$

$$\equiv SZn + H_2O \leftrightarrow \equiv SZnOH^- + H^+ \tag{2}$$

$$\equiv SZn + 2H^+ \leftrightarrow \equiv SH_2 + Zn^{2+} \tag{3}$$

In equations 3 to 5, $\equiv ZnS$ and $\equiv SZn$ denote the S and Zn atoms of the sphalerite surface, respectively. Because of the low solubility of sphalerite (Stanton et al., 2006), the reaction (5) was neglected in this study. The speciation diagrams from PHREEQC (Parkhurst and Appelo, 1999) software are shown in Fig. 1.
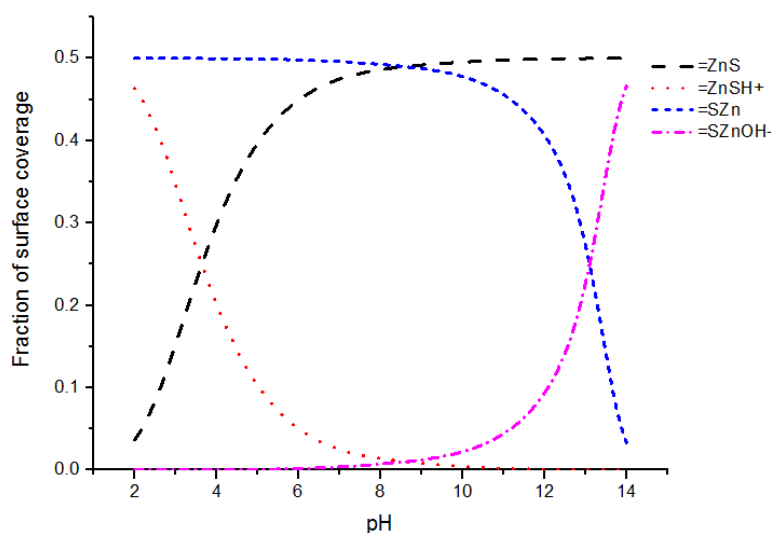

Fig. 1. Fractions of surface coverage of chemical groups in different pHs for sphalerite mineral

According to the fractions of surface coverage (as seen in Fig.1) the $-H^+$ and $-OH^-$ groups were placed on surface Zn and S sites, respectively. Cl anion and Na cation as counter-ions were placed near the surface functional groups for neutralizing the charge of surface. A vacuum slab with 100 Å thicknesses was considered for removing the mirror effect of water droplet. The model of surface was then optimized to equilibrate the surface functional group and counter-ions with slab. In separate model, amorphous cell tools were used to build a cube from 1000 molecule of water with the size of 31×31×31 angstroms. The SPC/E model was used for water model. After initial optimization, the cube was simulated under 100 picoseconds in the NVT ensemble and then 100 picoseconds in the NPT statistical ensemble, at the pressure of 1×10^{-4} GPa. After that, the periodic properties of the cell were removed and the molecules were simulated under 200 picoseconds in the NVT ensemble to form an equilibrium configuration of a droplet. Constructed droplet was then placed near the sphalerite surface with approximately equal distance from slab edges. After initially optimization of mineral-water droplet model, the NVT ensemble under 10^3 picoseconds duration with 1 fs time step at 298 K was performed. Results indicated that this simulation time is sufficient for water droplet to find an equilibrium shape with the surface. To measure contact angle after every 5×10^3 steps 1 frame was extracted. The contact angle was calculated for the last 20 frames of the MD simulation using the Hautman and Klein approach which were discussed in introduction.

Table 1. Energy components of Dreiding forcefield and related parameters for sphalerite mineral

Interaction	Equations	Terms	Descriptions	Parameters for sphalerite mineral		
Bond energy	$\sum_b \frac{1}{2}k_{ij}(R-R_0)^2$	R_0: the equilibrium bond length R : the current bond length k_{ij} : a specific constant which calculated for i and j atoms	The energy of a stretched or compressed bond between *i* and *j* atoms	k_{ij}	$\frac{kcal/mol}{Å^2}$	700
Angle energy	$\sum_\theta \frac{1}{2}k_\theta(\theta-\theta_0)^2$	: the equilibrium angleθ_0 : the current angleθ : a specific constant for the i, j and k k_θ atoms	The energy that arises from displacement of the angle formed by three atoms (i, j and k) from its equilibrium position.	k_θ	$\frac{kcal/mol}{Rad^2}$	100
Torsion energy	$\sum_\tau \sum_{n=1}^{p} \frac{1}{2}k_{\tau,n}[1-\cos(n\emptyset)]$	$k_{\tau,n}$: the force constant $\emptyset$: torsional angle n : is the periodicity (an integer)	The energy that arises from displacement of the $\emptyset$ angle formed by four atoms (i, j, k and l) from its equilibrium position.	$k_{\tau,n}$ n	$\frac{kcal}{mol}$ -	2 3
Inversion energy	$\sum_i \frac{1}{2}C(\cos\omega-\cos\omega_0)^2$	: inversion angleω : equilibrated angle between l-k bond ω_0 and plane made by i, j and k atoms	The energy arises from the displacement of an atom (l) from its equilibrium position to the mirror point in another side of plane made by i, j and k atoms.	C	$\frac{kcal/mol}{Rad^2}$	40
Electrostatic interactions	$\sum_{R_{ij}} C_0 \frac{Q_i Q_j}{\varepsilon_0 R_{ij}}$	Q_i and Q_j : charges on i and j atoms ε_0: is the dielectric constant C_0: overall columbic scaling factor; usually is taken as 332.0637 R_{ij} : distance between i and j atoms.	The interaction arises from the charges on i and j atoms.	**Q_i** and **Q_j** calculated from QEq approach		
Van der Waals interaction	$\sum_{R_{ij}} D_0\left[\left(\frac{R_0}{R_{ij}}\right)^{12} - 2\left(\frac{R_0}{R_{ij}}\right)^6\right]$	R_0 : the equilibrium distance D_0 : a specific constant for paired atoms. R_{ij} : distance between i and j atoms. the D_0 and R_0 values between unlike atoms are calculated from the values for the interaction between like atoms as following: $D_0^{ij}=\sqrt{D_0^{ii}D_0^{jj}}$ $R_0^{ij}=\sqrt{R_0^{ii}R_0^{jj}}$	The interaction arises from the correlations in the fluctuating polarizations of nearby the molecules and ions.	D_0 R_0	$\frac{kcal}{mol}$ Å	Zn 0.055 S 0.344 Zn 4.54 S 4.03
Hydrogen-bonding interaction	$\sum_{R_{ij}} D_0\left[5\left(\frac{R_0}{R_{ij}}\right)^{12} - 2\left(\frac{R_0}{R_{ij}}\right)^{10}\right]\cos^4\theta_{iHj}$	: the angle formed by i, H and j atoms.θ Other parameters are similar to the Van der Waals interaction.	When a hydrogen atom is boned to electronegative atoms such as (O, N, F, Cl and S) a strong tendency for attraction of molecules develops in the system which is known as hydrogen-bond interaction.	Same values presented in van der Waals interaction		

2.3 Shape characterizations of interface

The shape of droplet-substrate interface was sketch from the position of water molecules in outer layer of water droplet near the mineral surface (Fig. 2). The distance considered as the thickness of first layer of water molecules. Fig. 2.a shows the shape of water-sphalerite (110) interface, as can be seen the interface has a unsymmetrical shape, therefore ImageJ (Rasband, 1997) software was used to characterize the interface with shape factors such as: area (Fig. 2.b), perimeter (Fig. 2c) and Feret's (D_{Fmin} and D_{Fmax}) diameters (Fig. 2.d). As can be seen in Fig. 2e, the water-surface interface finds a preferred orientation in specific direction which can be considered as the effect of surface anisotropy on spreading of water droplet.

(a)   (b)   (c)   (d)   (e)
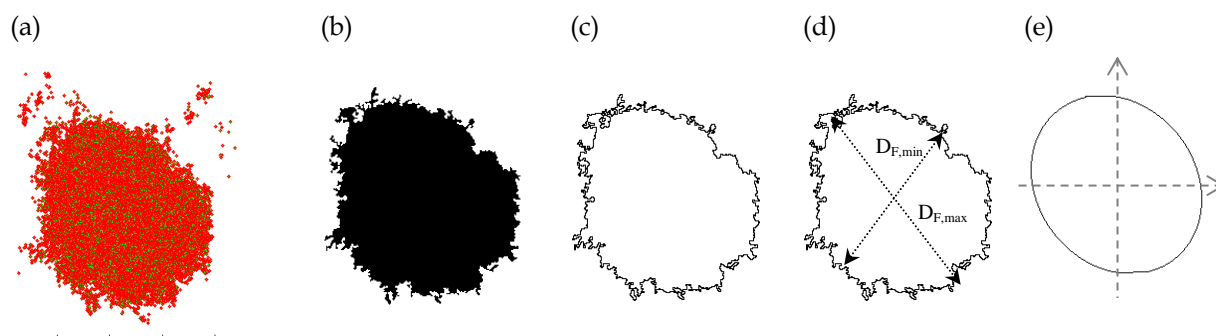

Fig. 2. a) Configuration of water droplet near the substrate surface (top view). b) water droplet interface area, c) perimeter, d) Feret's diameters and e) preferred orientation of water droplet-sphalerite interface

In this work, different spreading factors of water droplet on surface were defined at molecular level as following:

$$SF_1 = \frac{V}{A} \tag{1}$$

$$SF_2 = \frac{V}{P} \tag{2}$$

$$SF_3 = \frac{V}{D_F} \tag{3}$$

where V is the volume of water droplet, A is the area of droplet-surface interface, P is the perimeter of droplet-surface interface, and D_F is the Feret's diameters of interface. Using *angstrom* as length unit, spreading factors were calculated as *angstrom* for SF_1 and *angstrom²* for SF_2 and SF_3. Because of constant volume of water droplet (V) in molecular models, only the changes in shape characteristics of interface cause the change in spreading factors. Therefore, Correlations between the values of calculated contact angle and inverse of different shape factors were used to provide a good definition for spreading factor.

3. Results and discussions

3.1 Experimental and simulated contact angles

In order to assess the hydrophobicity of sphalerite surface, experimental contact angle of water droplet on sphalerite surfaces were measured. Conditioning of sphalerite surface in different pH was used to utilize different surface with different hydrophobicity. Table 2 presents the results obtained from the contact angle measurements of sphalerite surface after conditioning in specific pHs. As can be seen from the Table 2, the sphalerite surface has hydrophilic property ($\theta < 90$) in all pHs. It is apparent from this table that sphalerite exposes different hydrophilic properties in different pH. From this data, we can see that conditioning of surface at pH=6.50 resulted in the highest value of contact angle ($\theta = 53.4$ degree). The mean value for contact angles were 46.7 and 31.0 degrees for conditioning of surface at pH=9.00 and 10.57, respectively. There was a meaningful relation between increasing pH and hydrophobicity changes of the surface. In facts, formation of hydroxyl groups on sphalerite surface at higher pHs cause a significant decrease in contact angle and consequently decrease in surface hyrophobicity. Similar behaviors also were seen in mildly acidic and acidic conditions. In these cases, protonation of $\equiv$ ZnS sites on sphalerite surface according to the equation 3,

decreases the hydrophobicity of surface. Since the wetting property of a surface originated from the balance of adhesion and cohesion forces, so the experimental results suggest that there is an association between the formations of surface functional groups and wetting property of the surface. We calculated the contact angle of a water droplet on sphalerite surface from MD simulation to distinguish the effect of functional groups on wetting properties of ZnS (110) surface at molecular scale. Fig. 3 shows typical equilibrium snapshots of water droplet that is in contact with the sphalerite (110) surface. As can be seen in these images, the configuration of water droplets on surfaces were changed with progress in simulation time. Images in every column show the configuration of water droplet on sphalerite (110) surface with specific coverage of surface groups.

Table 2. Experimental contact angle of conditioned pure sphalerite surface with water droplet

pH	Experimental Contact angle (degree)	St. dev.
3.00	39.2	1.2
5.00	50.8	1.0
6.50	53.4	1.7
9.00	46.7	1.9
10.57	31.0	1.1

Table 3 provides the results obtained from the calculated contact angle at molecular scale. Data from this table can be compared with the data in Table 2 which shows the experimental contact angle values. This comparison reveals the effect of surface functional groups on wetting of sphalerite surface.

Table 3. Simulated contact angles of sphalerite (110) plane with water droplet

Surface composition Surface group (percentage of surface coverage)	Simulated Contact angle (degree)
SZn (50%) + ZnSH+ (50%)	28.7
SZn (50%) + ZnSH+ (25%) + ZnS (25%)	40.5
SZn (50%) + ZnS (50%)	50.1
SZn (25%) + SZnOH- (25%) + ZnS (50%)	39.5
SZnOH- (50%) + ZnS (50%)	24.8

It can be seen from the data in Table 3 that the sphalerite surface has the hydrophilic property ($\theta <$ 90) in all molecular simulations. Differences between measured and calculated contact angle have influenced by the difference between experimental and simulations conditions. Also, some physical characteristic such as surface morphology can affect the apparent hydrophobicity of surface in experimental measurements. Comparison of the simulated contact angle with those of experiment results confirms the reliability and accuracy of simulations for investigation on wetting changes of sphalerite in molecular scale. Near the neutral condition there is no protonated and hydroxylated sites on the sphalerite surface. The zero point of surface charge for sphalerite also happened near this conditions (pH=6.5) which indicate the surface is electrically neutral (Fuerstenau et al., 1974). In this condition, the sphalerite expose its higher hydrophobicity. Increasing in the surface coverage of both $\equiv ZnSH^+$ and $\equiv SZnOH^-$ groups on sphalerite surface causes a significant increase in hydrophilic properties of surface at simulations.

3.2 Shape characterization of droplet-surface interface

In simulations, it was initially observed that the water droplet has not a symmetrical shape as well as the droplet-substrate interface area. For characterization of shape properties of sphalerite-water interface image processing and analyzing were conducted to the shape of interface. Quantifying the
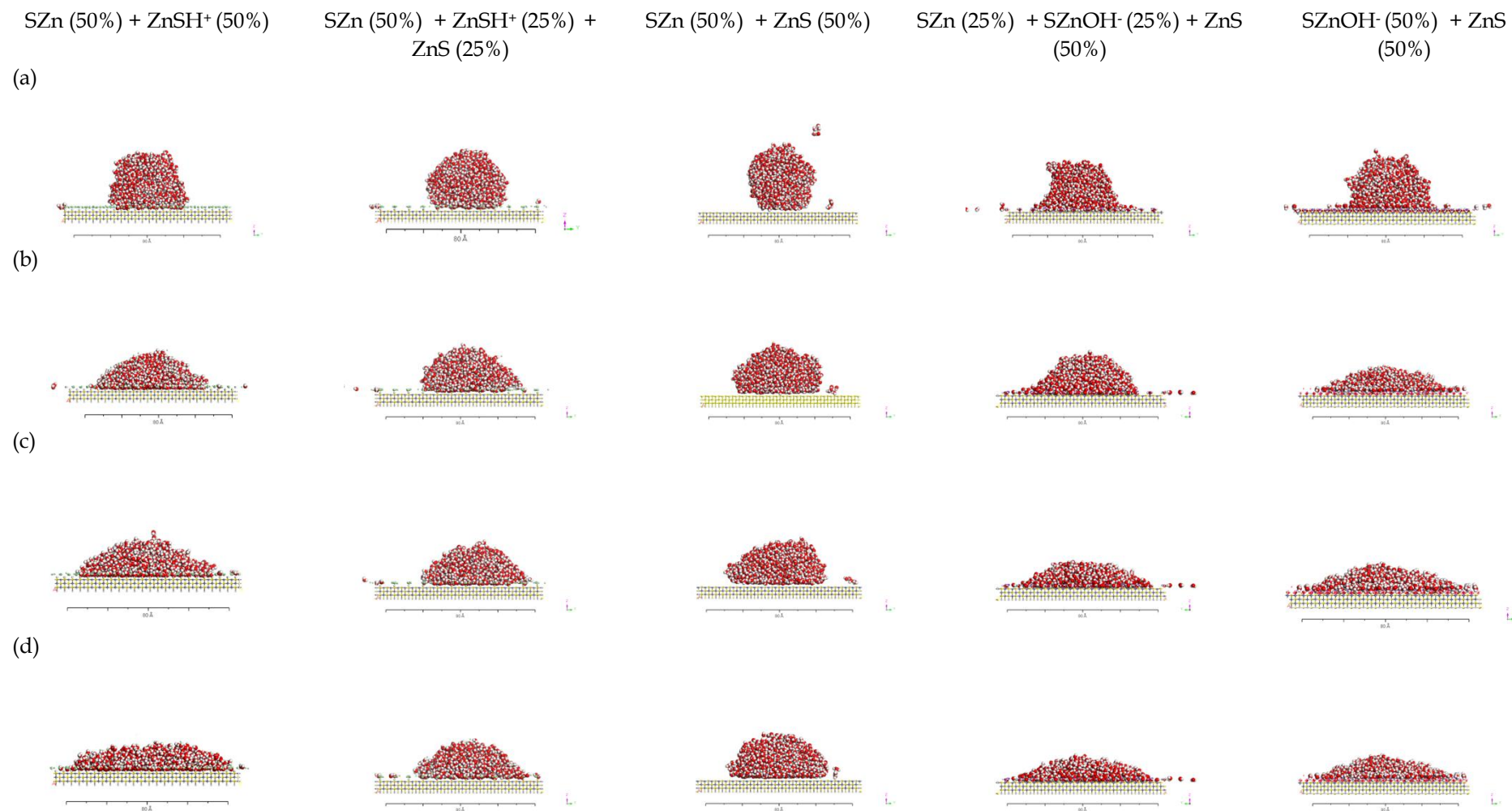
SZn (50%) + ZnSH⁺ (50%) SZn (50%) + ZnSH⁺ (25%) + SZn (50%) + ZnS (50%) SZn (25%) + SZnOH⁻ (25%) + ZnS SZnOH⁻ (50%) + ZnS
ZnS (25%) (50%) (50%)

(a)

(b)

(c)

(d)

Fig. 3. Configurations of water droplets on sphalerite (110) surface with different coverage of ZnSH⁺ and SZnOH⁻ groups. In every column: a) early stage, (b) and (c) transition stages to construct an equilibrium configuration of droplet on the surface, (d) late stage of wetting

shape of interface with some shape factors was used as an applicable approach to compare the geometry of droplet-substrate interface. The values of shape factors which were calculated for different systems are listed in Table 4.

Table 4. Geometrical properties and shape characterizations of water droplet- sphalerite (110) interface

Surface composition Surface group (percentage of surface coverage)	Perimeter (Å)	Area (Å²)	Feret's diameter (Å)		Circularity
			Min	Max	
SZn (50%) + ZnSH⁺ (50%)	458	3220	64.5	78.5	0.20
SZn (50%) + ZnSH⁺ (25%) + ZnS (25%)	323	2492	56.0	69.8	0.30
SZn (50%) + ZnS (50%)	265	1700	44.4	56.0	0.31
SZn (25%) + SZnOH⁻ (25%) + ZnS (50%)	452	2378	57.1	65.6	0.15
SZnOH⁻ (50%) + ZnS (50%)	626	4172	75.9	85.5	0.14

From Table 4, Feret's diameters and circularity values quantitatively indicate that the interface of the droplet and surface have not a symmetric shape. Because of low values for circularity factors (circ < 1), the interface of water surface has not a complete circular shape, therefore, in all simulations the minimum and maximum of Feret's diameters find different values. Since the volume of water droplet is equal for all calculated contact angles the spreading factors are only affected by the change in shape factors. The results of the correlational analysis between the simulated contact angle and inverse of the shape factors are presented in Table 5.

Table 5. Correlation coefficients between simulated contact angles and inverse of different shape descriptors

	$\dfrac{1}{\text{Perimeter}}$	$\dfrac{1}{\text{Area}}$	$\dfrac{1}{\text{Feret's diameter}}$	
			$\dfrac{1}{\text{Min Feret}}$	$\dfrac{1}{\text{Max Feret}}$
Simulated contact angle	0.92	0.98	0.97	0.97

Table 6. Calculated spreading factors of water droplet on sphalerite (110) surface with different surface composition

Surface composition Surface group (percentage of surface coverage)	$SF_1 = \dfrac{V}{A}$ (Å)	$SF_{3,max} = \dfrac{V}{\text{Min Feret}}$ (Å²)	$SF_{3,min} = \dfrac{V}{\text{Max Feret}}$ (Å²)
SZn (50%) + ZnSH⁺ (50%)	8.4	419	344
SZn (50%) + ZnSH⁺ (25%) + ZnS (25%)	10.8	482	387
SZn (50%) + ZnS (50%)	15.9	608	482
SZn (25%) + SZnOH⁻ (25%) + ZnS (50%)	11.4	473	412
SZnOH⁻ (50%) + ZnS (50%)	6.5	356	316

Correlation between the simulated contact angles and the (interface area)⁻¹ as well as the (perimeter)⁻¹ of the wetted zone declared a significant relation between the contact angle and calculated spreading factor of water droplet on surface. Surface with higher contact angle has the lower interface area and also lower perimeter of wetted zone; therefore, hydrophibic surfaces have a higher spreading factor than the hydrophilic surface. Positive correlations also were found between contact angles and (Feret's diameters)⁻¹. Comparing the results from Table 5, it can be seen that the contact angles of sphalerite surface have the correlation coefficient values of 0.98 with (interface area)⁻¹ while this value is 0.92 for correlation between the contact angles and (perimeter)⁻¹. From Table 5, correlation coefficient between contact angle and inverse of minimum and maximum of Feret's diameters is 0.97 which indicates that this shape descriptor also can be used in definition of spreading

factors at molecular scale. These findings suggest that the using of equations (6) and (8) for calculation of spreading factor is appropriate than the equation (7). The major advantage of the using Feret's diameters in calculation of spreading factor is that it calculates the maximum and minimum spreading factor in different direction and helps to distinguish the preferred orientation of water droplet at surface. The values of calculated spreading factors for sphalerite surface with different coverage of surface groups are presented in Table 6. From this data, we can see that using Feret's diameters two value of spreading factor in different direction are obtained while using the area only an overall spreading factor for water droplet on sphalerite surface is obtained.

4. Conclusions

In this work, we have demonstrated that the wetting behavior of a surface can be easily described with spreading factor of water droplet on substrate at molecular scale. This approach serves as a simple and fast tool for wetting comparison of different surface. Different definitions of spreading factors were examined and the most appropriate ones were selected for spreading factor calculations. Investigations on the wettability of sphalerite surface in experimental indicated that the sphalerite surface expose different wetting behavior in different pH. The contact angle was 53.4 degree for conditioned sphalerite at pH=6.50. The values of contact angle were 31.0 and 39.2 degrees at pH=10.57 and pH=3.00, respectively. Similar trend also was obtained from simulation of contact angle on sphalerite (110) plane with different coverage of functional groups. From MD simulation, the contact angles were 50.1 degree for surface without any $–H^+$ and $–OH^-$ groups. Increasing the surface coverage of $–H^+$ and $–OH^-$ groups resulted in decrease of contact angles to 28.7 and 24.8 degrees, respectively for protonated and hydroxylated surfaces. Correlational analysis indicated that obtained results from contact angle measurements can be justified by the results from spreading factor calculation. It was shown that spreading factors which were defined as the volume of water droplet divided by the area and Feret's diameters can be used to compare the wetting of different surface. Beside the comparison of the hydrophobicity of different surface, applying the spreading factor also indicated the preferable orientation of water droplet on a specific direction at molecular scale. The findings of this study suggest that the spreading factor can be used as a useful and simple method for fast and more accurate estimation on wettability characteristic of surfaces at molecular scale.

References

CARRÉ, A., EUSTACHE, F., 2000. *Spreading kinetics of shear-thinning fluids in wetting and dewetting modes*, Langmuir, 16, 2936-2941.

CHAU, T., 2009. *A review of techniques for measurement of contact angles and their applicability on mineral surfaces*, Minerals Engineering 22, 213-219.

CHAU, T., BRUCKARD, W., KOH, P., NGUYEN, A., 2009. *A review of factors that affect contact angle and implications for flotation practice*, Advances in colloid and interface science 150, 106-115.

CHEN, J., HANSON, B.J., PASQUINELLI, M.A., 2014. *Molecular dynamics simulations for predicting surface wetting*, AIMS Mater. Sci 1, 121-131.

CYGAN, R.T., KUBICKI, J.D., 2001. *Molecular modeling theory: Applications in the geosciences*, Mineralogical Society of America Washington, DC.

DE GENNES, P.-G., BROCHARD-WYART, F., QUÉRÉ, D., 2013. *Capillarity and wetting phenomena: drops, bubbles, pearls, waves,* Springer Science & Business Media.

DO HONG, S., HA, M.Y., BALACHANDAR, S., 2009. *Static and dynamic contact angles of water droplet on a solid surface using molecular dynamics simulation*, Journal of colloid and interface science 339, 187-195.

DU, H., MILLER, J.D., 2007. *A molecular dynamics simulation study of water structure and adsorption states at talc surfaces*, International Journal of Mineral Processing 84, 172-184.

EHLERS, W., GOSS, M., 2016. *Water dynamics in plant production*, CABI.

FAN, C.F., CAǦIN, T., 1995. *Wetting of crystalline polymer surfaces: A molecular dynamics simulation*, The Journal of chemical physics 103, 9053-9061.

FERRARI, M., LIGGIERI, L., MILLER, R., 2012. *Drops and bubbles in contact with solid surfaces*, CRC Press.

FORSLING, W., SUN, Z.-x., 1997. *Use of surface complexation models in sulphide mineral flotation*, International Journal of Mineral Processing 51, 81-95.

FRENKEL, D., SMIT, B., 2001. *Understanding molecular simulation: from algorithms to applications*, Academic press.

FUERSTENAU, M., CLIFFORD, K., KUHN, M., 1974. *The role of zinc-xanthate precipitation in sphalerite flotation*, International Journal of Mineral Processing 1, 307-318.

JIN, J., MILLER, J.D., DANG, L.X., WICK, C.D., 2015. *Effect of Cu 2+ activation on interfacial water structure at the sphalerite surface as studied by molecular dynamics simulation*, International Journal of Mineral Processing 145, 66-76.

KALINICHEV, A.G., 2014. *Molecular structure and dynamics of nano-confined water: Computer simulations of aqueous species in clay, cement, and polymer membranes*, Transport and Reactivity of Solutions in Confined Hydrosystems. Springer, pp. 103-115.

KALINICHEV, A.G., WANG, J., KIRKPATRICK, R.J., 2007. *Molecular dynamics modeling of the structure, dynamics and energetics of mineral–water interfaces: Application to cement materials*, Cement and Concrete Research 37, 337-347.

KOISHI, T., YASUOKA, K., FUJIKAWA, S., ZENG, X.C., 2011. *Measurement of contact-angle hysteresis for droplets on nanopillared surface and in the Cassie and Wenzel states: a molecular dynamics simulation study*, ACS nano 5, 6834-6842.

KRASOWSKA, M., ZAWALA, J., MALYSA, K., 2009. *Air at hydrophobic surfaces and kinetics of three phase contact formation*, Advances in colloid and interface science 147, 155-169.

MAYO, S.L., OLAFSON, B.D., GODDARD, W.A., 1990. *DREIDING: a generic force field for molecular simulations*, Journal of Physical chemistry 94, 8897-8909.

PARK, J.-Y., HA, M.-Y., CHOI, H.-J., HONG, S.-D., YOON, H.-S., 2011. *A study on the contact angles of a water droplet on smooth and rough solid surfaces*, Journal of Mechanical Science and Technology 25, 323-332.

PARKHURST, D.L., APPELO, C., 1999. User's guide to PHREEQC (Version 2): *A computer program for speciation, batch-reaction, one-dimensional transport, and inverse geochemical calculations*.

PAWLIK, M., 2008. *The surface properties of coal, Handbook of Surface and Colloid Chemistry*, Third Edition. CRC Press, pp. 655-680.

PRAT, M., 2007. *On the influence of pore shape, contact angle and film flows on drying of capillary porous media*, International journal of heat and mass transfer 50, 1455-1468.

RASBAND, W., 1997. *ImageJ software*. National Institutes of Health: Bethesda, MD, USA 2012.

SHAHRAZ, A., BORHAN, A., FICHTHORN, K.A., 2013, *Wetting on physically patterned solid surfaces: the relevance of molecular dynamics simulations to macroscopic systems*, Langmuir 29, 11632-11639.

SKINNER, B.J., 1961. *Unit-cell edges of natural and synthetic sphalerites*. the american mineralogist 46.

STANTON, M.R., TAYLOR, C.D., GEMERY-HILL, P.A., III, W.S., 2006. *Laboratory studies of sphalerite decomposition: applications to the weathering of mine wastes and potential effects on water quality*, 7th International Conference on Acid Rock Drainage (ICARD), p. 40502.

WANG, M., ZHANG, Q., HAO, W., SUN, Z.-X., 2011. *Surface stoichiometry of zinc sulfide and its effect on the adsorption behaviors of xanthate*, Chemistry Central Journal 5, 73.

WERDER, T., WALTHER, J.H., JAFFE, R.L., HALICIOGLU, T., NOCA, F., KOUMOUTSAKOS, P., 2001. *Molecular dynamics simulation of contact angles of water droplets in carbon nanotubes*, Nano Letters 1, 697-702.

WU, C.-D., KUO, L.-M., LIN, S.-J., FANG, T.-H., HSIEH, S.-F., 2012. *Effects of temperature, size of water droplets, and surface roughness on nanowetting properties investigated using molecular dynamics simulation*, Computational Materials Science 53, 25-30.

YAN, M., YANG, X., LU, Y., 2013. *Wetting behavior of water droplet on solid surfaces in solvent environment: A molecular simulation study*, Colloids and Surfaces A: Physicochemical and Engineering Aspects 429, 142-148.

YUAN, Q., ZHAO, Y.-P., 2013. *Wetting on flexible hydrophilic pillar-arrays*, Scientific reports 3, 1944.

YUAN, Y., LEE, T.R., 2013. *Contact angle and wetting properties, Surface science techniques*, Springer, pp. 3-34.

ZHANG, C., LIU, Z., DENG, P., 2016. *Contact angle of soil minerals: A molecular dynamics study*, Computers and Geotechnics 75, 48-56.

ZHANG, Q., XU, Z., FINCH, J.A., 1995. *Surface ionization and complexation at the sphalerite/water interface: I. Computation of electrical double-layer properties of sphalerite in a simple electrolyte*, Journal of colloid and interface science 169, 414-421.